Available online at www.sciencedirect.com
SCIENCE DIRECT®
Bioorganic & Medicinal Chemistry 12 (2004) 1995–2003
Bioorganic & Medicinal Chemistry

Kinetics and structure–activity relationship studies on pregnane-type steroidal alkaloids that inhibit cholinesterases

Asaad Khalid, Zaheer-ul-Haq, Shazia Anjum, M. Riaz Khan, Atta-ur-Rahman and M. Iqbal Choudhary*

Dr. Panjwani Center for Molecular Medicine and Drug Research, International Center for Chemical Sciences, University of Karachi, Karachi 75270, Pakistan

Received 20 December 2003; revised 25 February 2004; accepted 2 March 2004

Abstract—The mechanism of inhibition of acetylcholinesterase (AChE, EC 3.1.1.7) and butyrylcholinesterase (BChE, EC 3.1.1.8) enzymes by 23 pregnane-type alkaloids isolated from the *Sarcococca saligna* was investigated. Lineweaver–Burk and Dixon plots and their secondary replots showed that the majority of these compounds, that is **1**, **4**, **5**, **6**, **9**, **10**, **12**, **13**, **15**–**19**, and **21** were found to be noncompetitive inhibitors of both enzymes. Compounds **8**, **20**, **22**, and **23** were determined to be uncompetitive inhibitors of BChE, while compounds **11** and **14** were found to be uncompetitive and linear mixed inhibitors of AChE, respectively. K_i values were found to be in the range of 2.65–250.0 μM against AChE and 1.63–30.0 μM against BChE. The structure–activity relationship (SAR) studies suggested that the major interaction of the enzyme–inhibitor complexes are due to hydrophobic and cation–π interactions inside the aromatic gorge of these cholinesterases. The effects of various substituents on the activity of these compounds are also discussed in details.

1. Introduction

The most important and well-documented function of AChE is the hydrolysis of the neurotransmitter acetylcholine.[1] This enzyme has long been an attractive target for rational drug design and discovery of mechanism-based inhibitors for the treatment of Alzheimer's disease (AD), Parkinson's disease and myasthenia gravis. On the other hand, the physiological function of BChE is still unclear. However, it has been found that the BChE is present in significantly higher quantities in Alzheimer's plaques than in plaques of normal age-related nondemented brains.[2] Moreover, AChE is known to accelerate the aggregation of β-amyloid peptide during the early stages of AD. This feature of AChE was shown to be inhibited by the noncompetitive peripheral site binding inhibitors of AChE, but not by the competitive active site binding inhibitors. Interestingly, BChE, which lacks some key amino acids in its peripheral site is not known to promote the β-amyloid formation.[3]

The aromatic gorge of both cholinesterases possess four subsites that are involved in molecular recognition and catalysis. The AChE aromatic gorge includes the following loci:

(1) The acyl-binding locus in which the enzyme–ligands interactions give rise to the acetyl specificity.[1,4] This might involves close contacts between the bound inhibitor and the side-chains of Gly-119, Trp-233, Phe-288, Phe-290, and/or Phe-331.
(2) The esteratic locus, which consists of two subsites, (a) the oxyanion hole in which the oxyanionic oxygen of the inhibitor (if any) is situated among three convergent NH bonds from residues Gly-118, Gly-119, and Ala-201,[5] and (b) The active site catalytic triad, which comprise on amino acids Ser-200, Glu-327, and His-440 and interacts with the cationic substrates such as ACh. The esteratic locus of the aromatic gorge also interacts with hydrophobic substrates and ligands.[6,7]
(3) Quaternary ammonium binding locus; in which the quaternary ammonium functionality of many ligands interacts with the side chains of Trp-84,

Keywords: Steroidal alkaloids; *Sarcococca saligna*; Acetylcholinesterase; Butyrylcholinesterase; Inhibition; SAR; Kinetic studies.
* Corresponding author. Tel.: +92-21-9243211/9243224; fax: +92-21-9243190/91; e-mail addresses: hej@cyber.net.pk; zainraa@digicom.net.pk

0968-0896/$ - see front matter © 2004 Elsevier Ltd. All rights reserved.
doi:10.1016/j.bmc.2004.03.002

Glu-199, and Phe-330, and the phenolic oxygen of Tyr-130. These residues form a concave-type binding site that recognizes the quaternary ammonium function.[5]

(4) The peripheral site;[1,4] also called as peripheral anionic site, situated >10 Å above the active site triad and near the opening of the aromatic gorge. The peripheral site of AChE includes Tyr-70, Asp-72, Tyr-121, Glu-278, Tyr-334, and Trp-279 residues.[8–10] Ligand occupation of the peripheral anionic site therefore allosterically changes the conformation of the active center.[9,11]

The recently solved crystal structure of BChE[3] was shown to be very similar to that of electric eel AChE. However, several aromatic groups of residues lining the gorge of the AChE, have been replaced in BChE by hydrophobic ones. Moreover, the acyl-binding pocket of BChE, contains Leu-286 and Val-288 instead of Phe-288 and Phe-290 of AChE, makes it possible for BChE to accommodate bulkier substrates and ligands. BChE and Chicken AChE, lacks Trp-279. This results in a greatly reduced binding of bisquaternary peripheral site ligands to BChE.[12]

Since the current AChE inhibitors are still far from perfection, the interests and efforts in the discovery of novel AChE inhibitors are expected to continue in future. As part of our ongoing investigations on the cholinesterases inhibition by natural products, we now describe the detailed cholinesterases inhibitory activity, inhibition kinetics and the structure–activity relationship (SAR) of a series of steroidal alkaloids **1**–**23**, which were previously isolated and identified as new cholinesterases inhibitors by us from *Saraccoca saligna*.[13,14] This series includes, salignenamide-C (**1**), salignenamide-D (**2**), 2β-hydroxyepipachysamine-D (**3**), salignenamide-E (**4**), salignenamide-F (**5**), axillarine-C (**6**), axillarine-F (**7**), sarcorine (**8**), N_a-demethylsaracodine (**9**), saligcinnamide (**10**), salignenamide-A (**11**), vaganine-A (**12**), 5,6-dehydrosarconidine (**13**), 2-hydroxysalignarine-E (**14**), salignamine (**15**), 2-hydroxysalignamine-E (**16**), epipachysamine-D (**17**), dictyophlebine (**18**), iso-*N*-formaylchonemorphine (**19**), sarcodinine (**20**), axillaridine-A (**21**), sarsalignone (**22**), and sarsalignenone (**23**). The purpose of this study is mainly to develop a better understanding of the SAR in this new class of cholinesterases inhibitors.

2. Results and discussion

Pregnane-type steroidal alkaloids have steroidal skeleton with monomethylamino or dimethylamino substituents either at C-3 and/or at the C-20 position in basic steroidal skeleton. These compounds contain various substituents, which play an important role in the inhibitory activities of these compounds against cholinesterases. For instance, compounds **14** and **16** contain amino substituent only at C-20 position, while rests of compounds reported in this study have amino substituents at both C-3 and C-20 positions. Compounds **1**–**3**, **6**, **7**, **14**, **16**, and **19** have hydroxyl group at C-2 position, while compounds **1**, **6**, **7**, and **12** have acetoxy substituent at C-3 position. The structures of the compounds reported in this study are shown in Chart 1.

Electric eel AChE was used in this study because of two reasons; firstly, the oligometric forms of AChE in the electric eel is structurally similar to those in AChE of vertebrates, nerve, and muscles.[15,16] Secondly the results obtained with this enzyme allow molecular modeling studies to be conducted using the coordinates of the published eel AChE X-ray structure.[15] Similarly, horse serum BChE used in this study has similarities with synaptic acetylcholinesterase in primary amino acid sequence, deduced secondary structure, and active site chemistry. The two enzymes also have overlapping specificities for substrates and inhibitors.[17]

The K_i values (the dissociation constant of the enzyme–inhibitor complex into free enzyme and inhibitor), IC_{50} values (the concentrations of test compounds that inhibits the enzyme activity by 50%) and type of inhibition of AChE and BChE enzymes by alkaloids **1**–**23** are listed in Table 1. The graphical analysis of steady state inhibition data for some of the active compounds against AChE and BChE is presented in Figures 1–4.

Determination of the inhibition type is critical for identification of the mechanism of inhibition and the site(s) of inhibitor binding. The classical noncompetitive inhibitor and the substrate bind reversibly, randomly and independently at different sites on the enzyme. On the other hand, classical uncompetitive inhibitor does not bind to the free enzyme, but binds reversibly to the enzyme–substrate complex, yielding an inactive complex. This inhibition is an example of the sequential order of binding of two ligands to the enzyme in an obligate order. Therefore, substrate binding is considered necessary to produce conformational changes in the enzyme, which creates or opens the inhibitor binding site.

The majority of the compounds, as shown in Table 1, exhibited a pure noncompetitive type of inhibition as they decrease the V_{max} values without affecting the affinity of the enzyme toward the substrate (K_m values). The purity of the inhibition was determined by the secondary replots of Lineweaver–Burk plots as these plots show linear lines. The graphical analysis of steady state inhibition data of compound **23** for AChE and compound **12** for BChE is shown in Figs. 1 and 2, respectively, as example of this type of inhibition.

Unlike all other compounds of this series, AChE showed high K_m and low V_{max} values in the presence of compound **11** (Fig. 3), indicating a linear mixed type of inhibition. This type of inhibition is generally the result of combination of partially competitive and pure noncompetitive inhibitions. The partial competitive nature of inhibition by compound **11** was further confirmed by the replot of Dixon (Fig. 3B), in which the line does not cross the origin unlike pure competitive inhibition. Meanwhile the pure noncompetitive nature was inferred from the decrease in V_{max} value and unambiguously

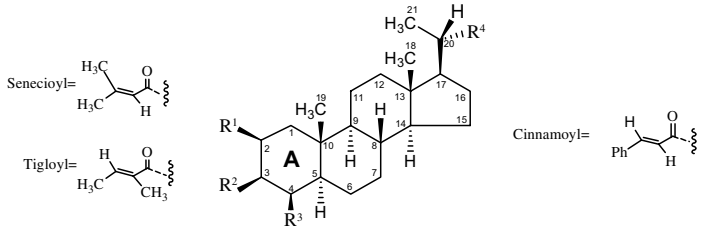

Compound	R^1	R^2	R^3	R^4	Unsaturation
Salignenamide-C (**1**)	OH	*HN-Tigloyl*	OAc	$N(CH_3)_2$	$\Delta^{14,15}$
Salignenamide-D (**2**)	α-OH	*HN-Tigloyl*	H	$N(CH_3)_2$	$\Delta^{4,5}$& $\Delta^{16,17}$
2β-Hydroxyepipachysamine-D (**3**)	OH	*HN-Benzoyl*	H	$N(CH_3)_2$	
Salignenamide-E (**4**)	H	$NCH_3COCH{=}CCH_3CH(CH_3)_2$	H	$N(CH_3)_2$	$\Delta^{16,17}$
Salignenamide-F (**5**)	H	$NCH_3COCH{=}CCH_3CH(CH_3)_2$	H	$N(CH_3)_2$	
Axillarine-C (**6**)	OH	*HN-Benzoyl*	OAc	$N(CH_3)_2$	
Axillarine-F (**7**)	OH	*HN-Tigloyl*	OAc	$N(CH_3)_2$	
Sarcorine (**8**)	H	*N*HAc	H	$N(CH_3)_2$	
N_a-Demethylsaracodine (**9**)	H	$NHCH_3$	H	NCH_3Ac	
Saligcinnamide (**10**)	H	CH_3N *-Cinnamoyl*	H	$N(CH_3)_2$	
Salignenamide-A (**11**)	H	$NHCOCH{=}C(CH_3)CH(CH_3)_2$	H	$N(CH_3)_2$	
Vaganine-A (**12**)	H	*HN-Senecioyl*	OAc	$N(CH_3)_2$	
5,6-Dehydrosarconidine (**13**)	H	$NH(CH_3)$	H	$N(CH_3)_2$	$\Delta^{16,17}$
2-Dydroxysalignarine-E (**14**)	OH	OCH_3	H	$N(CH_3)_2$	$\Delta^{5,6}$& $\Delta^{16,17}$
Salignamine (**15**)	H	OCH_3	H	$N(CH_3)_2$	$\Delta^{5,6}$& $\Delta^{16,17}$
2-Hydroxysalignamine-E (**16**)	OH	*HN-Tigloyl*	H	$N(CH_3)_2$	$\Delta^{4,5}$
Epipachysamine-D (**17**)	H	*HN- Benzoyl*	H	$N(CH_3)_2$	
Dictyophlebine (**18**)	H	$NHCH_3$	H	$N(CH_3)_2$	
Iso-*N*-formylchoneformine (**19**)	OH	$N(CH_3)_2$	H	*NHCHO*	
Sarcodinine (**20**)	H	$N(CH_3)_2$	H	$N(CH_3)_2$	$\Delta^{5,6}$

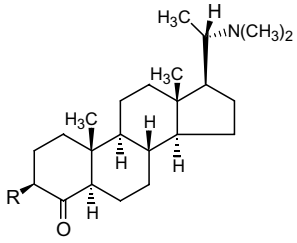

Compound	R	Unsaturation
Axillaridine-A (**21**)	*HN-Benzoyl*	$\Delta^{2,3}$
Sarsalignone (**22**)	*HN-Tigloyl*	$\Delta^{5,6}$
Sarsalignenone (**23**)	*HN-Tigloyl*	$\Delta^{5,6}$ & $\Delta^{14,15}$

Chart 1. Chemical structures of steroidal alkaloids **1**–**23**.

confirmed by the secondary replots of Lineweaver–Burk plots, which yielded straight lines characteristic of noncompetitive inhibition (Fig. 3D). The increase in K_m value indicated that the compound **11** causes a decrease in the substrate affinity toward the active site of the enzyme. This suggested that the compound **11** might be inducing certain conformational changes in the enzyme's structure by binding with the enzyme–substrate complex. This can eventually decrease the activity of the enzyme. This suggested that the inhibitor and the substrate are not mutually exclusive and both bind independently to each other.

Compounds **8**, **20**, **22**, and **23** showed an interesting uncompetitive type of inhibition of BChE, as they decrease both the K_m and V_{max} values. Compound **23** provides an example of the graphical data fitting of these four compounds since they all show similar Lineweaver–Burk plots, Dixon plots, and their secondary replots (Fig. 4). Interestingly these four compounds were found to be noncompetitive inhibitors of AChE as described earlier.

In order to establish the relationships between chemical structures and kinetic behavior of these steroidal alkaloid inhibitors of AChE and BChE, the following considerations have been applied:

1. Since these compounds were found to be either noncompetitive, uncompetitive or linear mixed inhibitors of both cholinesterases, it was predicted that the inhibitors bind at (or satisfactorily close to) the aromatic gorge in the presence or absence of substrate. The alternate possibility of off-gorge binding, which requires massive conformational change with aromatic gorge disruption, was not considered since the reactions catalyzed by inhibited enzyme progressed linearly.

Table 1. In vitro cholinesterases inhibitory activities of compounds **1**–**23**

Compound	Acetylcholinesterase			Butyrylcholinesterase		
	IC_{50} (μM)[a]	K_i[b] (μM)[a]	Inhibition	IC_{50} (μM)[a]	K_i[b] (μM)[a]	Inhibition
1	61.3 ± 2.02	134 ± 6.58	NC	38.36 ± 2.75	26.3 ± 1.44	NC
2	185.2 ± 7.66	—	—	23.78 ± 0.16	—	—
3	78.2 ± 2.33	—	—	28.96 ± 0.01	16.2 ± 0.14	NC
4	6.21 ± 0.23	10.7 ± 0.19	NC	3.65 ± 0.023	9.1 ± 0.26	NC
5	6.35 ± 0.22	4.1 ± 0.06	NC	4.07 ± 0.108	3.4 ± 0.09	NC
6	227.9 ± 8.67	126 ± 9.71	NC	17.99 ± 0.22	20.3 ± 0.67	NC
7	182.4 ± 5.54	—	—	18.24 ± 0.25	—	—
8	69.99 ± 2.6	90.3 ± 2.03	NC	10.33 ± 0.21	7.5 ± 1	UC
9	204 ± 4.95	216 ± 4	NC	16.55 ± 0.20	15 ± 0.4	NC
10	19.99 ± 0.12	12.2 ± 0.15	NC	4.84 ± 0.12	6.6 ± 0.15	NC
11	50.64 ± 0.93	9.05 ± 0.25	LM	4.63 ± 0.073	3.25 ± 0.20	NC
12	8.59 ± 0.16	17.6 ± 0.2	NC	2.32 ± 0.06	2.58 ± 0.02	NC
13	20.29 ± 1.82	14.2 ± 0.15	NC	1.89 ± 0.06	1.75 ± 0.03	NC
14	249 ± 10.3	250 ± 9.19	UC	25.7 ± 0.63	30 ± 1.26	NC
15	82.5 ± 2.22	70 ± 3.06	NC	20.95 ± 3.2	29 ± 0.9	NC
16	15.99 ± 0.13	16 ± 0.73	NC	6.91 ± 0.06	7 ± 3.15	NC
17	28.93 ± 0.54	29.2 ± 0.54	NC	2.82 ± 0.02	5.36 ± 0.13	NC
18	6.21 ± 0.23	10.7 ± 0.19	NC	3.65 ± 0.023	9.1 ± 0.26	NC
19	6.357 ± 0.22	4.1 ± 0.06	NC	4.07 ± 0.11	3.4 ± 0.09	NC
20	40.04 ± 0.13	42 ± 0.73	NC	12.51 ± 0.06	13 ± 3.15	UC
21	5.21 ± 0.11	3.03 ± 0.03	NC	2.49 ± 0.06	2.15 ± 0.25	NC
22	7.02 ± 0.01	5.4 ± 0.05	NC	2.18 ± 0.04	3.08 ± 0.55	UC
23	5.83 ± 0.07	2.65 ± 0.08	NC	4.29 ± 0.029	1.63 ± 0.41	UC
Eserine	0.041 ± 0.001	0.014 ± 0.001	MT	0.857 ± 0.01	0.9 ± 0.05	NC
Tacrine	0.021 ± 0.002	0.23 ± 0.02	MT	0.051 ± 0.005	0.025 ± 0.003	MT
Galanthamine	0.45 ± 0.02	0.19 ± 0.01	MT	39.1 ± 0.032	32 ± 0.33	NC

NC = noncompetitive, UC = uncompetitive, LM = linear mixed, MT = mixed type, — = Not tested due to insufficient quantities.
[a] IC_{50} and K_i values are expressed as (mean ± SEM), where SEM is the standard mean error of three experiments.
[b] K_i is the mean of four values calculated from Lineweaver–Burk plot, its secondary replots, and Dixon plot.

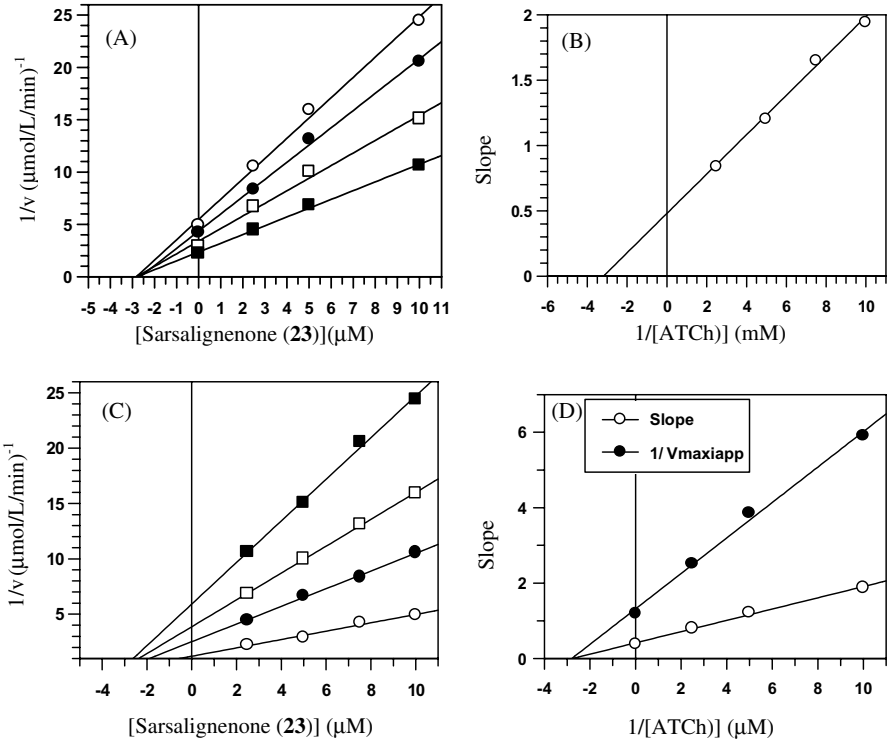

Figure 1. Steady state inhibition of AChE by sarsalignenone (**23**). (A) Dixon plot at four fixed ATCh concentrations: (○) 0.1 mM; (●) 0.13 mM; (□) 0.2 mM and (■) 0.4 mM. (B) Respective secondary replot of the Dixon plot: slope versus reciprocal of the ATCh conc. (C) Lineweaver–Burk plot in absence (○) and presence of 2.5 μM (●), 5 μM (□), and 10 μM (■) of compound **23**. (D) Secondary replots of the Lineweaver–Burk plot: $1/V_{maxi}$ or slope versus various concentrations of inhibitor.

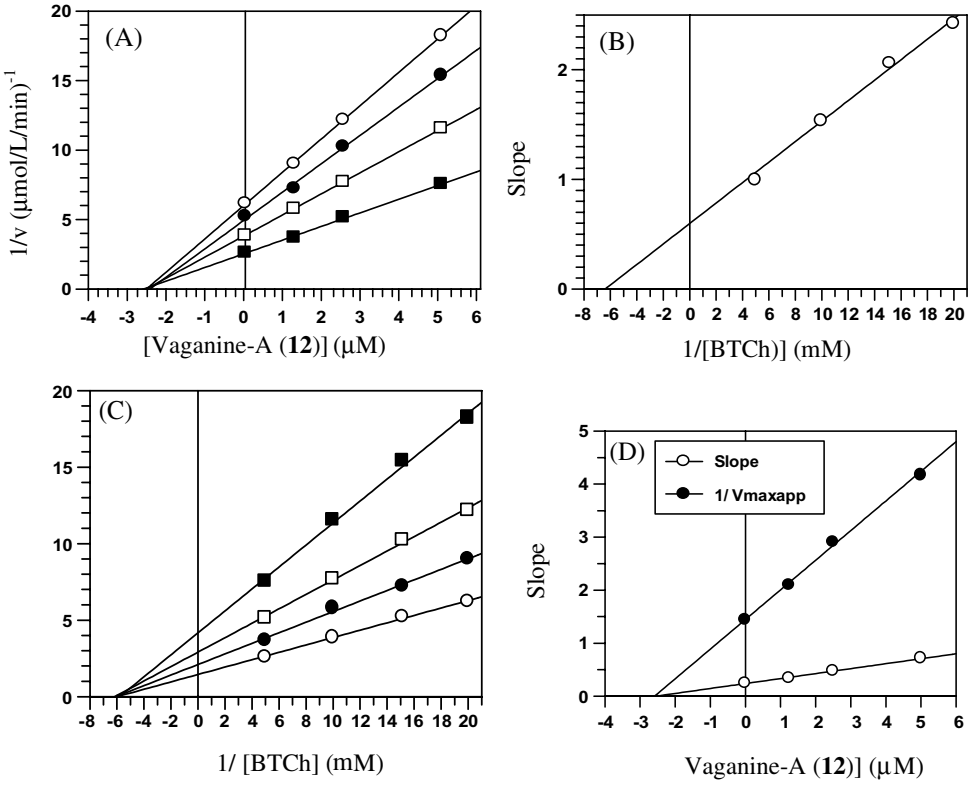

Figure 2. Steady state inhibition of BChE by vaganine-A (**12**). (A) Dixon plot at four fixed BTCh concentrations: (○) 0.05 mM; (●) 0.06 mM; (□) 0.1 mM and (■) 0.2 mM. (B) Respective secondary replot of the Dixon plot: slope versus reciprocal of the BTCh. (C) Lineweaver–Burk plot in absence (○) and presence of 1.25 µM (●), 2.5 µM (□), and 5 µM (■) of compound **12**. (D) Secondary replots of the Lineweaver–Burk plot: $1/V_{maxi}$ or slope versus various concentrations of inhibitor.

2. Like most proteins, AChE is conformationally flexible. However, in the absence of any evidence that AChE readily undergoes extensive conformational changes which disrupt the aromatic gorge, a conservative view of the enzyme and aromatic gorge was taken for SAR studies and minimal conformational changes, if any, were assumed.

The data in Table 1 suggests that various functional groups and substitutions pattern did produce a remarkable variation in the activities. The SAR results of this study is discussed below.

We suggest here that the polycyclic compounds may penetrate the aromatic gorge with ring A being first to enter. This could be due to the more hydrophobic character of ring A, and/or due to the increased electropositivity of ring A substitutions. Moreover, since most of the ligands binding sites lie near the bottom of the aromatic gorge of the cholinesterases enzymes rather than the surface of the gorge, this could also explain the greater influence of C-3 amino substituents as compared to C-20 amino substituents on the activity of the compounds.

The structures of alkaloids **1**–**23** show clearly that the amino nitrogens at C-3 and/or C-20 positions are the most important structural features that determine the inhibitory potency of these compounds. This is due to the fact that the nitrogens at C-3 and/or C-20 positions are expected to be protonated at physiological pH and thus can mimic the quaternary nitrogen of some known quaternary and bisquaternary inhibitors binding at the peripheral site of the enzyme.

It is also noteworthy that the large negative charge of AChE aromatic gorge helps in binding the cationic ligands and acetylthiocholine (ATCh) (and also by analogy the physiological substrate ACh) to the enzyme surface area, which is sometime larger than the active site itself and proceeds to the active site by diffusion on the surface of the enzyme.[1] The electrical field of AChE/BChE is therefore thought to accelerate the rate of binding of quaternary ammonium ligands to the aromatic gorge of the enzyme. However, affinity labeling, computer docking, site-directed mutagenesis, and structural studies of complexes of AChE with quaternary and bisquaternary ligands such as decamethonium showed that such ligands lie along the gorge.[5,9–10,15,18–20] One quaternary group is closer to Trp-84 residue, which is an the important constituent of the anionic subsite of the aromatic gorge. The other quaternary group has been inferred to be closer to the top of the gorge near several aromatic amino acids, such as Trp-279, Tyr-70, and Tyr-121.[9,19–22]

According to the results of kinetic studies, the position of C-3 and C-20 amino groups in alkaloids **1**–**23** in the aromatic gorge of AChE is not expected to bridge the two anionic sites of the enzyme. C-20 amino group may

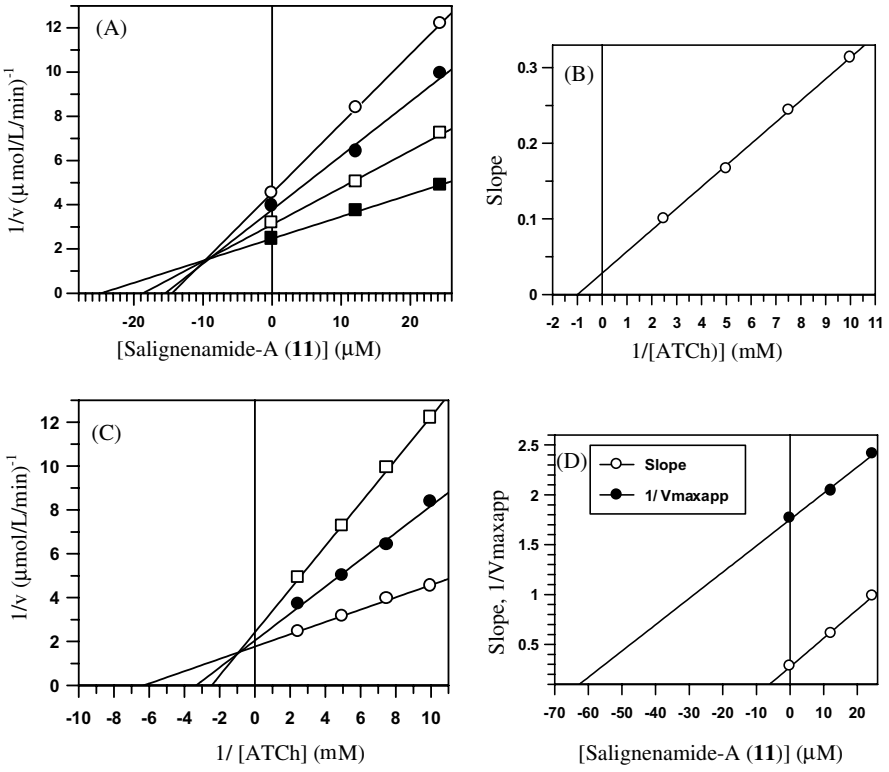

Figure 3. Steady state inhibition of AChE by salignenamide-A (**11**). (A) Dixon plot at four fixed ACh concentrations: (○) 0.1 mM; (●) 0.13 mM; (□) 0.2 mM and (■) 0.4 mM. (B) Respective secondary replot of the Dixon plot: slope versus reciprocal of the ATCh. (C) in absence (○) and presence of 12.5 µM (●) and 25 µM of compound **11**. (D) Secondary replots of the Lineweaver–Burk plot: $1/V_{maxapp}$ or slope versus various concentrations of inhibitor.

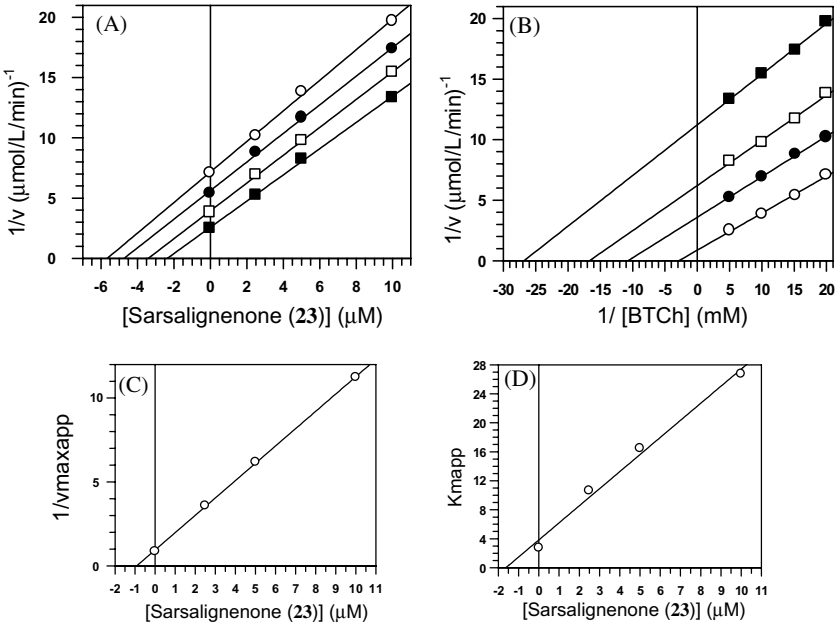

Figure 4. Steady state inhibition of BChE by sarsalignenone (**23**). (A) Dixon plot at four fixed ATCh concentrations: (○) 0.05 mM; (●), 0.06 mM; (□) 0.1 mM and (■), 0.2 mM. (B) Lineweaver–Burk plot in absence (○) and presence of 2.5 µM (●), 5 µM (□) and 10 µM (■) of compound **23**. (C) and (D) Secondary replots of the Lineweaver–Burk plot: $1/V_{maxapp}$ and K_{mapp} versus various concentrations of inhibitor, respectively.

remain close to the aromatic rings of Tyr-70 and Trp-279, near the top of the gorge, thus allowing the substrate to be accommodated at the active site of the enzyme.

Bergmann and Segall have shown that a critical separation of the quaternary centers of the compounds is necessary to obtain an enhanced inhibition.[23] Thus, a

distance of approximately 14 Å (corresponding to 10–12 carbons chain) between the quaternary centers, seems optimal for the agonist action. However, when minimized 3D models were constructed for the compounds under study, the distances between the two amino groups (i.e. at C-3 and C-20) were found to be in the range of 12.7–12.9 Å. This distance apparently is not as long as it is in some other bisquaternary inhibitors (such as decamethonium), which can interact with the enzyme by cation–π interactions between the amino groups and the Trp-84 and Trp-279 residues of the two anionic sites of the aromatic gorge of AChE enzyme.

The results of mutagenesis of Trp-84 conducted by Ordentlich et al.[24] indicate that cation–π and dispersion interactions are important molecular recognition elements in the quaternary ammonium binding locus. However, the quaternary ammonium function interacts with the π electron faces of Trp-84 and Phe-330. Therefore, it is obvious that cation–π interactions between the amino groups of the alkaloids **1**–**23** and the Trp-279, Tyr-70 and Tyr-121 residues could be one of the major stabilizing factors in the AChE-inhibitor complex.

This finding was further supported by the fact that the replacement of any of these two amino substituents with oxygen function, as in compounds **14** and **15**, exhibit decrease in the IC_{50} and K_i values against AChE. It is, however, interesting to note that the presence of an oxygen function at C-3 of steroidal alkaloids did effect the potency of these compounds against both cholinesterases.

Except compounds **9** and **19**, all other steroidal alkaloids of this series have amidic functions at the C-3 position. These substituents may provide them additional stabilization beside the cation–π and the hydrophobic interactions. It is, however, not clear what these stabilizing factors are. This could partially explain why compound **9** was far less potent inhibitor of AChE as compared to the other compounds.

The most active members of this series were found to be compounds **21**–**23**. They have a carbonyl or acetoxy substituents at C-4. This suggests a possible role of these substituents in the activity of these compounds. All these compounds were found to be noncompetitive inhibitors of AChE. Moreover, all these compounds were also found to be potent inhibitors of BChE. The carbonyl group at the C-4 position of the compound may bind with residues of the peripheral site such as Tyr-121.

Benzamide moieties at C-3 of compounds **3**, **6**, and **17** appears to cause a steric hindrance, which may result in some decrease in the activity, as compared to the compounds containing aliphatic side chain such as tigloyl or sencioyl groups at C-3. The steric effect of C-3 benzamide substituent may be due to the limited possible flexibility of the molecule within the aromatic gorge of the enzyme. The orientation of the molecule may have a strong impact on the hydrophobic interactions between the enzyme and inhibitor. Interestingly, when the sencioyl and tigloyl groups are present at C-3 of compounds (as in compounds **7**, **14**, **16**, **22**, and **23**), these compounds exhibited similar inhibitory activities against AChE and BChE.

On the other hand, the key substituents, which may negatively affect the inhibitory activity against both the AChE and BChE include C-2 hydroxyl or C-2 acetoxy groups. For example, the activity of compounds **1**, **2**, **3**, **7**, **8**, **14**, and **16** is fairly low against both enzymes. Moreover, all these compounds were found to be the noncompetitive inhibitors of enzymes. This demonstrates the influence of the C-2 hydroxyl or acetoxy substituents on the activity and mechanisms of action of these compounds. Although, compound **19** contains a hydroxyl group at C-2, it still shows a comparatively better activity profile against both cholinesterases. This compound was the only member of this series with aldhydic group at C-20.

The negative effect of C-2 hydroxy or C-2 acetoxy substituents on the inhibitory activity might be due to some unfavorable interactions, which counteract with the usual stabilizing factors such as hydrophobic or electrostatic interactions. Compounds **2**, **3**, **7**, and **14** were found to be the least active members of this series indicating that the C-2 hydroxyl group is the major negative factor on the activities of these compounds.

This preliminary study indicates that the affinity of the compounds, which are bulkier than the most known cholinesterases inhibitors, could be rationalized in part by the flexibility of these compounds due to rotation around single bonds and due to the multiple interactions contributing to the stabilization of the enzyme–inhibitor complexes.

The dimensions of the aromatic gorges of the cholinesterases are adequate in size to fully accommodate all inhibitors included in this study. This was shown by the crystal structures of both enzymes and further supported by our on going docking studies, which will be published somewhere else (Fig. 5). However, since the diffusion of aromatic gorge binding ligands including substrate ACh to the aromatic gorge is probably rate determining,[1] it can be assumed that these compounds would have more potent activity if they are smaller in size. This could also explain why all these compounds were found to be more selective toward BChE, which has a wider aromatic gorge as compared to AChE.

So far all the known cholinesterases inhibiting drugs used in Alzheimer's disease suffer from several major drawbacks such as high toxicity, short duration of biological action, low bioavailability, and narrow therapeutic windows. This demands further research in this field to discover new inhibitors with better pharmacological properties. This new series of cholinesterases inhibitors therefore, may act as potential leads in the discovery of clinically useful agents for various nervous system disorders including memory impairment in

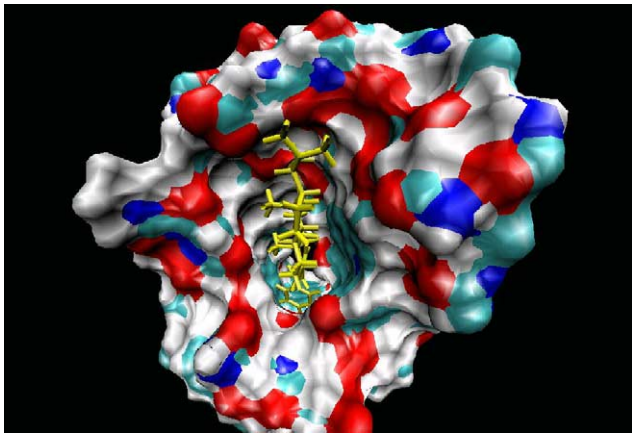

Figure 5. Axillaridine-A (**21**) is shown to be fully buried inside the aromatic gorge of AChE enzyme. Only the amino acid residues between 10 Å are shown for clarity.

Alzheimer's patients by potentiating and affecting the cholinergic transmission process.[25]

3. Experimental section

3.1. General inhibition assays

AChE and BChE inhibitory activities were determined in vitro by a modified spectrophotometric method developed by Ellman et al.[26] All inhibition studies were performed in 96-wells micro titer plates, using Spectra-Max microplate spectrophotometer (Molecular Devices, CA, USA).

Electric eel AChE (type VI-S, Sigma), and horse serum BChE (Sigma) were used, while acetylthiocholine iodide and butyrylthiocholine chloride (Sigma) were used as substrates in the reactions. Ellman reagent that is 5,5-dithiobis (2-nitro) benzoic acid (DTNB, Sigma) was used to develop the chromogenic marker for the measurement of the cholinesterases activity. All the other reagents and conditions and the assay procedure were same as described previously,[13] All the reactions were performed in triplicate and the initial rates were measured as the rate of change in OD/min (optical density/min) and used in subsequent calculations.

According to Ellman et al. since the extinction coefficient of the yellow anion is known, the rate of the enzymatic reaction can be calculated by the following equation.[26]

$$\text{Rate (mols/L/min)} = \frac{\text{change in absorbance/min.}}{13,600}$$

3.2. Estimation of inhibition constants

Two different methods were applied to monitor the effect of the inhibitor (test sample) on both K_m and V_{max} values. This was done firstly by plotting the reciprocal of the rate of the reactions against the reciprocal of the substrate concentration as Lineweaver–Burk plot, and secondly by the Dixon plot in which the reciprocal of the rate of the reactions was plotted against the inhibitor concentrations.[27] The secondary replots of the Lineweaver–Burk were also constructed in two ways; firstly, $1/V_{maxi}$ were determined at each intersection point of every inhibitor concentration line on the y-axis of Lineweaver–Burk plot and then replotted against different concentrations of the respective inhibitor. Secondly, in the case of the noncompetitive and linear mixed-type inhibitions, the slope of each line of inhibitor concentration on Lineweaver–Burk plot was plotted against inhibitor concentrations. For the uncompetitive type of inhibition, K_{mapp} was determined from the intersection of the inhibitor concentrations lines on the x-axis of Lineweaver–Burk plot and plotted against inhibitor concentrations. The secondary replot of Dixon plot was constructed as the slope of each line of substrate concentration in original Dixon plot against the reciprocals of the substrate concentrations.

K_i values (the dissociation constant of the dissociation of the enzyme–inhibitor complex into free enzyme and inhibitor) were determined by the interpretation of Dixon plot, Lineweaver–Burk plot, and its secondary replots by using initial velocities. These velocities were obtained over a range of substrate concentrations between 0.1 and 0.4 mM for ATCh and 0.05 and 0.2 mM for BTCh. The assay conditions for measurement of the residual activities of all inhibitors were identical to the aforementioned spectrophotometric assay procedure except that fixed concentrations of inhibiting compounds were used in the assay medium.

The types of inhibition were determined by the graphical views of Dixon plots, Lineweaver–Burk plots and their secondary plots.

3.3. Statistical analysis

All assays were conducted in triplicate. Graphs were plotted using GraFit program.[28] Values of the correlation coefficient, slope, intercept and their standard errors were obtained by the linear regression analysis using the same software. The correlation coefficient for all the lines of all graphs was >0.99, each point in the constructed graphs represents the mean of three experiments.

Acknowledgements

The authors wish to thank The Ministry of Science and Technology, Government of Pakistan for providing the financial assistance under the Pak-Kazakh scientific cooperation program. We are extremely grateful to Dr. Rafat A. Siddiqui, Indiana University, Indianapolis, USA, for kind assistance and cooperation. We are also

thankful for Prof. Alan Harvey, Strathclyde Institute for Drug Research, University of Strathclyde, Glasgow, UK, for reviewing the manuscript of this paper.

References and notes

1. Quinn, D. M. *Chem. Rev.* **1987**, *87*, 955.
2. Yu, Q.; Holloway, H. W.; Utsuki, T.; Brossi, A.; Greig, N. H. *J. Med. Chem.* **1999**, *42*, 1855.
3. Nicolet, Y.; Lockridge, O.; Masson, P.; Fontecilla-Camps, J. C.; Nachon, F. *J. Biol. Chem.* **2003**, *278*, 41141.
4. Massoulie, J.; Pezzementi, L.; Bon, S.; Krejci, E.; Vallette, F. M. *Prog. Neurobiol.* **1993**, *41*, 31.
5. Harel, M.; Quinn, D. M.; Nair, H. K.; Silman, I.; Sussman, J. L. *J. Am. Chem. Soc.* **1996**, *118*, 2340.
6. Rosenberry, T. L. *Adv. Enzymol. Relat. Areas. Mol. Biol.* **1975**, *43*, 103.
7. Rosenberry, T. L.; Bernhard, S. A. *Biochemistry* **1972**, *11*, 4308.
8. Radic, Z.; Duran, R.; Vellom, D. C.; Li, Y.; Cervenansky, C.; Taylor, P. *J. Biol. Chem.* **1994**, *269*, 11233.
9. Shafferman, A.; Velan, B.; Ordentlich, A.; Kronman, C.; Grosfeld, H.; Leitner, M.; Flashner, Y.; Cohen, S.; Barak, D.; Ariel, N. *EMBO J.* **1992**, *11*, 3561.
10. Barak, D.; Kronman, C.; Ordentlich, A.; Ariel, N.; Bromberg, A.; Marcus, D.; Lazar, A.; Velan, B.; Shafferman, A. *J. Biol. Chem.* **1994**, *269*, 6296.
11. Radic, Z.; Quinn, D. M.; Vellom, D. C.; Camp, S.; Taylor, P. *J. Biol. Chem.* **1995**, *270*, 20391.
12. Eichler, J.; Anselmet, A.; Sussman, J. L.; Massoulie, J.; Silman, I. *Mol. Pharmacol.* **1994**, *45*, 335.
13. Atta-ur-Rahman; Zaheer-ul-Haq; Khalid, A.; Anjum, S.; Khan, M. R.; Choudhary, M. I. *Helv. Chim. Acta* **2002**, *85*, 678.
14. Atta-ur-Rahman; Zaheer-ul-Haq; Feroz, F.; Khalid, A.; Nawaz, S. A.; Khan, M. R.; Choudhary, M. I. *Helv. Chim. Acta*. **2004**, *87*, 439.
15. Sussman, J. L.; Harel, M.; Frolow, F.; Oefner, C.; Goldman, A.; Toker, L.; Silman, I. *Science* **1991**, *253*, 872.
16. Bon, S.; Vigny, M.; Massoulie, J. *Proc. Natl. Acad. Sci. U.S.A.* **1979**, *76*, 2546.
17. Chatonnet, A.; Lockridge, O. *Biochem. J.* **1989**, *260*, 625.
18. Barak, D.; Ordentlich, A.; Bromberg, A.; Kronman, C.; Marcus, D.; Lazar, A.; Ariel, N.; Velan, B.; Shafferman, A. *Biochemistry* **1995**, *34*, 15444.
19. Weise, C.; Kreienkamp, H. J.; Raba, R.; Pedak, A.; Aaviksaar, A.; Hucho, F. *EMBO J.* **1990**, *9*, 3885.
20. Harel, M.; Schalk, I.; Ehret-Sabatier, L.; Bouet, F.; Goeldner, M.; Hirth, C.; Axelsen, P. H.; Silman, I.; Sussman, J. L. *Proc. Natl. Acad. Sci. U.S.A.* **1993**, *90*, 9031.
21. Sussman, J. L.; Harel, M.; Silman, I. In *Multidisciplinary Approaches to Cholinesterase Functions*; Shafferman, A., Velan, B., Eds.; Plenum: New York, 1992; pp 95–107.
22. Vellom, D. C.; Radic, Z.; Li, Y.; Pickering, N. A.; Camp, S.; Taylor, P. *Biochemistry* **1993**, *32*, 12.
23. Bergmann, F.; Segal, R. *Biochem. J.* **1954**, *58*, 693.
24. Ordentlich, A.; Barak, D.; Kronman, C. *J. Biol. Chem.* **1995**, *270*, 2082.
25. Guillozet, A. L.; Smiley, J. F.; Mash, D. C.; Mesulam, M. M. *Ann. Neurol.* **1997**, *42*, 909.
26. Ellman, G. L.; Courtney, K. D.; Andres, V., Jr.; Featherstone, R. M. *Biochem. Pharmacol.* **1961**, *7*, 88.
27. Dixon, M. *Biochem. J.* **1953**, *55*, 170.
28. Leatherbarrow, R. J., 4.09 ed.; Erithacus Software Ltd.: Stains, UK, 1999.